Field Response of an Instrumented Dyke Subjected to Rainfall

A. Jotisankasa[1], S. Pramusandi[2], S. Nishimura[3] and S. Chaiprakaikeow[4]
[1,2,3]*Department of Civil Engineering, Kasetsart University, Bangkok, Thailand*
[3]*Division of Field Engineering for the Environment, Hokkaido University, Sapporo, Japan*
E-mail: fengatj@ku.ac.th

ABSTRACT: A field study was undertaken of an instrumented dyke on soft Bangkok clay in Pathumthani, Thailand. The studied site was characterised using dynamic cone penetration tests, field vane shear tests and Spectral Analysis of Surface Waves geophysical tests. The pore-water pressure, suction, moisture content and rainfall were continuously monitored over the rainy season in 2017. The soft clay nearer the dyke had higher strength than in the zone further away due to consolidation. The upper 0.5 m of dyke fill material made up of silty and clayey soils were found to experience drastic suction changes, reaching 1800 kPa towards the end of a drought and abruptly reducing to 20-40 kPa within a day upon the onset of the rainy season. Such large and abrupt changes of the suction are likely to have aggravated the surface cracking and hence the dyke movements. In contrast, the response at 3 m depth from the dyke shoulder was almost insensitive to the short-term rainfall patterns. Vertical movement of the dyke surface showed compression-swelling phenomena, probably due to the combined effects of drying, collapse-on-wetting and swelling and suggested that some movement is recoverable. This was not the case for horizontal movements, which exhibited constant outwards cumulative displacement.

KEYWORDS: Dyke, Slope, Pore-water pressure, Suction, Rainfall, Instrumentation

1. INTRODUCTION

Dykes or levees are the crucial part of a flood defence system and their stability and integrity during service life are of great importance. In many countries, rapid urbanisation, ground subsidence and sea level rising mean that an increasingly large numbers of dykes will be built, upgraded and require more extensive maintenance. In most cases, extreme precipitation and floods cause major collapses of dykes (Sills et al., 2007, Duc et al., 2017). Extreme drought has been reported to cause weakening of dykes (Robinson & Vahedifard, 2016, Vahedifard et al., 2016). This has led to a number of studies aimed at better understanding dyke behaviour and their response to climatic factors (Van Baars , 2005, Karl et al., 2008, Nishimura et al., 2015, Vahedifard et al., 2017, Fern et al., 2017, Jasim & Vahedifard, 2017)

The low-lying floodplain in central Thailand (including the capital Bangkok) regularly experiences floods during the rainy season. Extensive development of residential areas and industrial estates within these provinces, notably, Ayutthaya and Pathumthani, have necessitated the construction of polders (a system of embankments or dykes used to protect an enclosed area from flooding) as part of the flood defence system for such areas. Many rural roads, constructed decades ago, have also been heightened by placing fill on the surface so they could also function as dykes during flooding. In particular, the 2011 great flood in Thailand brought about complete inundation and breaching of many of these dykes. Consequently, this incident led to further reinforcing and heightening of the dyke or construction of permanent concrete pile walls to prevent future flooding. Nevertheless, the severe drought in Thailand in 2015 caused widespread slope failure in many sections along these heightened roads and dykes. Extreme climatic patterns, involving heavy rainfall and severe drought clearly play a crucial role in dyke stability in Thailand.

The influence of climate on dyke is complex, depending on various factors, such as soil type, soil profile, precipitation, evapotranspiration, topography, as well as vegetation cover. Information is needed on behavioural changes in dykes in relation to climate to improve the design, construction and maintenance of existing and future dykes. A number of studies have been reported on the field performance of natural or fill slopes in the tropics which provided insights into the pore water pressure regime and suction changes in relation to rainfall (e.g. Tsaparas et al., 2003, Jotisankasa et al., 2015). Nevertheless, the response of dykes to climatic factors in tropical countries is rarely reported in the literature. The negative pore-water pressure in dykes is expected to play an important role on desiccation cracks on the dyke surface during a prolonged drought which is likely to happen as a result of climate change. Extreme cycles of drying and wetting could contribute to dyke excessive movement and failure. Thus, the study on negative pore-water pressure is of importance and relevance on improving design and maintenance of future dykes and upgrading of existing dykes in the current climatic condition.

In addition to this, the negative pore water pressure plays a role even during flooding. Depending on the dyke size, the positive pressure due to inundation does not necessarily propagate to the dyke core or the other side within 1-2 days with the kind of low-permeability soil commonly used to construct dykes. The remaining negative pressure contributes to the stability. This effect is normally assessed in practice in seepage analysis by inputting both the rainfall and flooding. The study on dyke suctions is important in understanding the pre-flooding initial conditions for such analysis.

This paper investigated the field responses of an instrumented dyke in Pathumthani, Thailand. The studied site was characterised using three in situ tests (dynamic cone penetration test, field vane shear test and Spectral Analysis of Surface Waves (SASW) geophysical test). The pore-water pressure, suction, moisture content along the slope and rainfall were continuously monitored over a rainy season in 2017. The slope deformation was measured using total station survey. The dyke's visual appearance was continuously monitored using an action camera. A relationship was qualitatively explored between slope deformation and pore-water pressure change.

2. SITE CHARACTERISATION

2.1 Asian Institute of Technology dyke

The studied site was a 10 m long section of the dyke on the northern side of the Asian Institute of Technology (AIT) in Pathumthani, Thailand (Figure 1). The dyke system had been built to form a polder, consisting of the AIT, National Science and Technology Development Agency (NSTDA) and Thammasat University (TU). This study site was chosen based on its representativeness of clay dykes in central Thailand, site accessibility and protection of equipment from vandalism. An additional benefit was that the site had normally a low traffic volume so that the effects of traffic surcharge on the dyke response could be justifiably ignored in the analysis. A minor longitudinal crack along the crest of the studied section was observed at the beginning of site survey in 2016, indicating slope movement was likely. Desiccation cracks were also found along the slope surface in the middle and the top parts during the dry season. The studied section of the dyke was about 3m above the original

ground level with a side slope of about 1:1.7 (V:H) as measured in 2017.

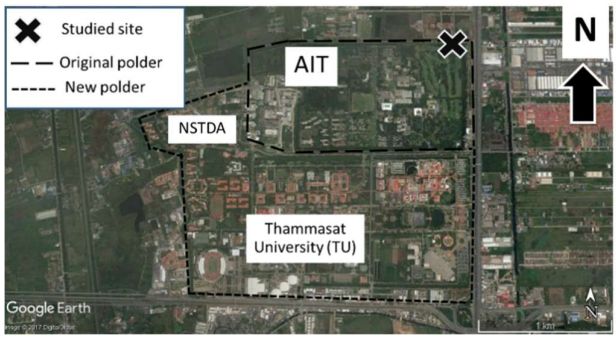

Figure 1 Location of studied dyke at AIT and approximate location of polder (Source: Google Earth 2017)

The AIT dyke of the original polder was first built in the late 1960's with an original height of 1.5-2 m in the northern section. During the 2011 flood, the northern and eastern parts of the original dyke were overtopped and breached by the tremendous amount of flood water, leaving the AIT and Thammasat campuses and NSTDA inundated by about 3 m of water. In response to this incident, the dyke was heightened by about 1 m to an elevation of +4.291 m above mean sea level (ASL) in 2012 by placing lateritic fill on top of the original dyke. About 0.5 m thickness of desiccated softened material at the top of original dyke was scraped off before placing the new fill. A slope geometry survey using a total station instrument was carried out at the study site to construct cross-sections of the dyke as presented in Figure 2. Notably, in May 2017, the water level in the canal outside the polder was about 50cm higher than that on the AIT side.

2.2 Ground profile and in-situ tests

Disturbed samples were collected from the AIT side of the dyke using hand-augers and test pits from the surface to 2 m depth for basic property tests. Table 1 summarises the grain size distribution, liquid limit (LL), plasticity index (PI) and soil types according to the Unified Soil Classification System (USCS) for all the soil layer units as shown in Figure 2. The upper part of the dyke consisted of Unit-1, the road surface made of a layer of crushed rock and lateritic granular soil of about 55 cm thickness, overlying Unit-2, the upper clay fill consisting of low-plasticity clay (CL). The middle part of the dyke fill consisted of Unit-3, upper silty clay fill classified as low-to-high- plasticity clay (CL, CH) and low-plasticity silt (ML) and Unit-4, lower silty fill, consisting of low-plasticity silt (ML) and silty sand (SM). Unit-5, the upper crust, and Unit-6, the lower crust consisted of low-plasticity silt (ML) and high-plasticity silt (MH), and had similar properties. The soft clay, Unit-7, was classified as high plasticity clay (CH).

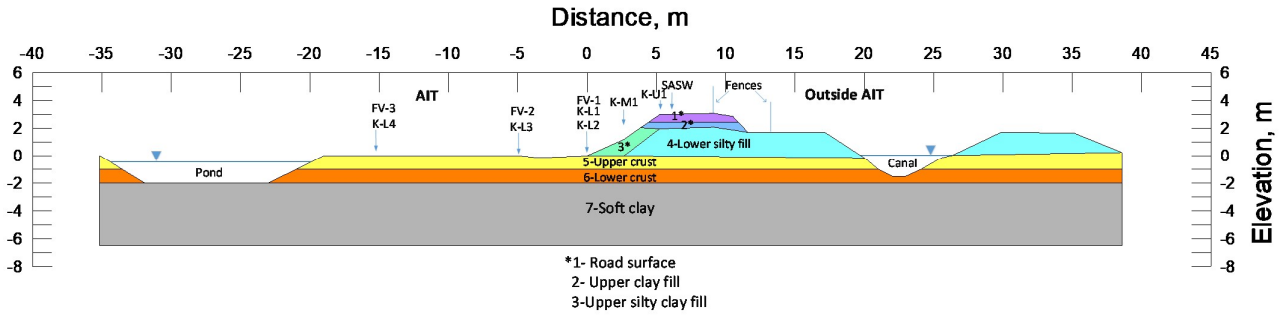

Figure 2 Cross-section of the instrumented AIT dyke (water level in pond at 9 May 2017)

Table 1 Summary of basic soil properties

Soil unit	% Gravel, >4.75 mm	% Sand, 0.075 - 2 mm	% Silt, 0.075 -5μm	% Clay, <5μm	LL, %	PI	USCS
1-Road surface	16.6-34.7	62-80	3.2-7.3	0.8-1.2	31.9-52.2	11.5-24.0	SP, SW-SC
2-Upper clay fill	12.1	22.8	23.9	41.3	43.8	22.4	CL
3-Upper silty clay fill	2.3-4.24	13.6-17.6	37.8-50.3	29.7-44.3	48.6-50.3	19-24.4	CL/CH, ML
4-Lower silty fill	4.8-11.4	48.4-75.7	13.0-46.8	2.3-3.4	47.4-48.0	14.5-20.6	ML, SM
5-Upper crust	0.0	2.7-5.0	49.1-53.5	43.8-45.9	48-52.5	17.1-21.4	ML, MH
6-Lower crust	0.0	1.1-2.1	45.8-54.8	43.2-53.1	47.7-53.4	15.6-21.8	ML, MH
7-Soft clay*	-	10-30	20-30	50-70	60-75	30-40	CH

*Source: Horpibulsuk et al. (2007)

A series of in situ tests were performed to characterise the ground profile on the AIT side of the dyke. Field vane shear tests at 3 locations (FV-1, FV-2 and FV-3 as shown in Figure 2) were conducted to characterise the soft clay layer from a depth of 2 m up to 7 m, beyond which the medium-to-stiff clay layer was encountered. The tests used a GEONOR H-10 device according to ASTM-D 2573–01. Variations of both peak and remoulded undrained shear strength along with the sensitivity are plotted in Figure 3. The peak undrained shear strength, s_u, for locations FV-1 and FV-2, which were near the dyke toe, followed a similar trend, being relatively constant with depth (20-25kPa). However, the peak s_u values for location FV-3, which was 15 m outside the dyke area, was somewhat lower, ranging between 7 and 17 kPa. The FV-3 shear strength likely represents the strength of original ground, before dyke construction. The clay nearer the dyke toe (FV-1 and FV-2) would have consolidated as a result of dyke fill after the original dyke was built about 50 years ago, and the additional fill was placed in 2012. The clay near the dyke is therefore of higher peak strength. The remoulded strength was of similar value for all locations, indicating similar intrinsic properties. The thickness of the soft clay is only about 4-5 m at this site. The clay is classified as moderately-sensitive to sensitive, and of similar sensitivity value for all three locations, ranging from 3 to 9. This trend is in a good agreement with previous studies on Bangkok clay (e.g. Horpibulsuk et al., 2007, Mairaing & Amonkul, 2010)

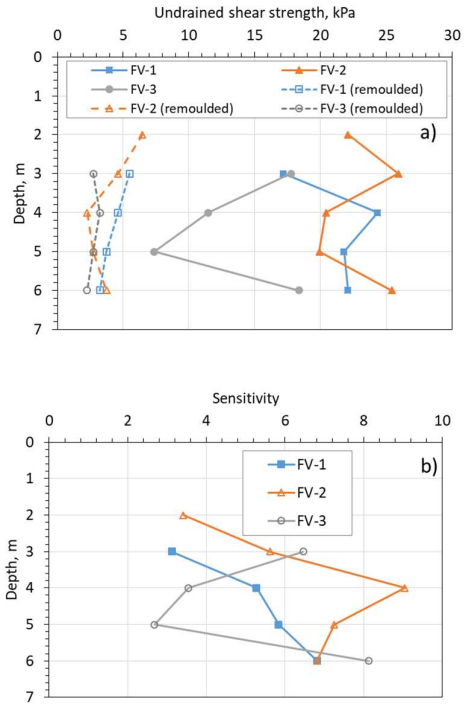

Figure 3 Field vane shear test results

The crust zone of the Bangkok clay is a weathered medium-stiff to a stiff clay. This crust layer, as well as the dyke fill have been characterised by means of light-weight dynamic cone penetration test, or so-called Kunzelstab Penetration test (KPT). This test involves dropping a 10 kg weight, with a falling height of 0.5 m, on a 60° cone with a diameter of 25 mm connected to 20 mm diameter rod. The number of blow counts was recorded for each 20 cm of penetration. The KPT has been carried out at six locations (K-U1, K-M1, K-L1, K-L2, K-L3, and K-L4 as shown in Figure 2) on the AIT side of the dyke. Figure 4 shows the plots of blow counts versus depth for all locations. The blow count number appeared to be fairly constant up to 1.5 m depth below which it started to increase linearly with depth. Notably, the KPT resistance (blow count number) below 1.5 m depth was likely affected by the skin friction in the soft clay along the rod above that depth. The presence of soft clay was confirmed by the SASW results, presented in the following section.

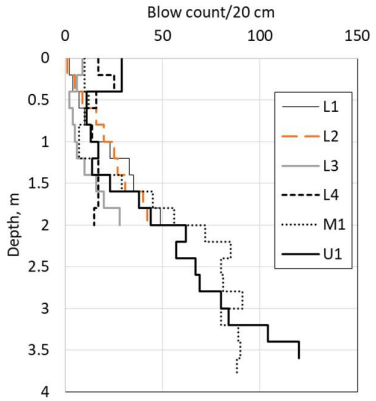

Figure 4 Kunzelstab Penetration test (KPT) results

Thus, the blow count number appeared to increase with depth, indicating a larger accumulated skin friction along the depth in the soft clay. Nevertheless, the upper crust zone from zero to 1 m depth appeared softer nearer the dyke (L1 and L2) than outside (L3 and L4), likely due to ground depression near the toe (Figure 2).The lower crust zone from 1 to 2 m depth at Location L4, outside of Dyke area, appeared softer (lesser blow count) than crust beneath the dyke.

A contour plot of blow counts has been constructed as shown in Figure 5. Evidently, the upper 1 m of the crust zone and dyke fill were softer than the lower 1 m of the crust and fill. The soil profile shown in Figure 2 was drawn based on these observations. The upper 1 m of dyke fill on the side slope appeared to have a smaller shear resistance, as compared to the lower part, likely because it was only recently placed during dyke upgrading in 2012. It could also be so because the influence of rain infiltration into desiccation crack that would be more intensive in the upper 1 m of the slope.

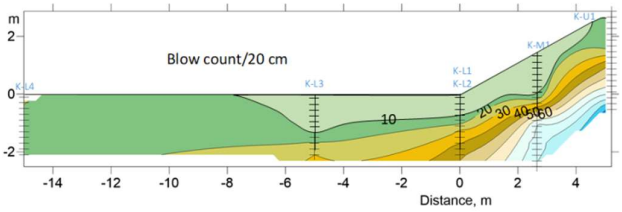

Figure 5 Contour of KPT blow counts

2.3 Spectral Analysis of Surface Waves (SASW) Testing

Spectral Analysis of Surface Waves (SASW) testing, the technique developed by the University of Texas at Austin (Nazarian et al., 1983, Stokoe et al., 1994), was performed at the crest of the dyke in order to measure the shear wave velocity of the dyke and the soil foundation. The test was performed using a sledgehammer and a 300-kg drop weight as a seismic source for shallow and deep profile investigations, respectively. The receivers were two 2-Hz geophones manufactured by Geospace. The arrangements of the source and receivers were the Common Receiver Midpoint geometry for short spacing (1, 2 and 5 m) and the Common Source geometry for long spacing (10 and 20 m), due to the difficulty in relocating the drop weight. The results from these spacings were combined to determine the shear wave velocity profile using WinSASW program, also developed by the University of Texas at Austin (Joh, 1996). The combined experimental and theoretical dispersion curves are shown in Figure 6. The shear wave velocity profile, evaluated from iterative forward modelling analysis, of the site is shown in Figure 7. Soil properties are also shown in Table 2.

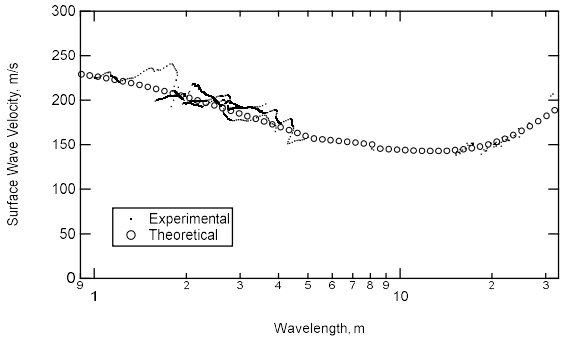

Figure 6 Experimental and theoretical dispersion curves of AIT dyke

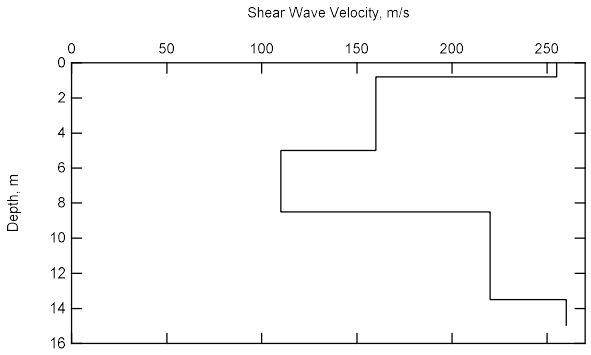

Figure 7 Shear Wave Velocity Profile measured from AIT Dyke

Table 2 Layer Properties Determined from SASW Test at AIT Dyke

Depth to Top of Layer, m	Layer Thickness, m	Shear Wave Velocity, m/s	Assumed Values P-Wave Velocity, m/s	Poisson's Ratio	Mass Density, tons/m^3
0	0.8	255	477	0.3	2
0.8	4.2	160	299	0.3	1.8
5	3.5	110	1500	0.497	1.7
8.5	5	220	1500	0.489	2
13.5	1.5*	260	1500	0.485	2

The result indicates the shear wave velocity of 160-255 m/s in the first 5m representing the embankment and the top crust materials. It, then, drops down to 110 m/s for the next 3.5m representing the thickness of soft Bangkok clay. After that the velocity becomes higher than 220 m/s representing much stiffer soils. The undrained shear strength of the soft soil was estimated using Equation 1 developed by Ashford et al. (1996) where v_s = shear wave velocity (in m/s) and s_u is an undrained shear strength (in kN/m^2).

$$v_s = 23 s_u^{0.475} \quad (1)$$

The estimated undrained shear strength is about 27 kPa which is slightly higher than what was measured by field vane shear test. However, it is worthwhile to note that the field vane shear test was carried out at the dyke toe while the SASW was performed at the crest. Therefore the soft clay tested by field vane shear test would have experienced lower overburden pressure comparing to the soft clay tested by SASW test which has experienced higher overburden pressure due to the weight of the dyke.

While it is true the penetration resistance and the stiffness should show a good correlation, and hence similar profiles, the compatibility between the KPT blow count profile (Figure 4) and shear wave velocity profile (Figure 7) cannot be strictly discussed due to inherent difference in the test principles, resolution and range of measurement of the two tests. The KPT was conducted on a small amount of soil (a local measurement), while the SASW test was on a much larger amount of soil (a global measurement) and showed the averaged shear wave velocity of the soil mass. The KPT result presents a profile over 3.6 m at a 0.2 m resolution, while the SASW result extends down to 16m depth but at a resolution of 1-4 m. In addition, the KPT resistance at a depth greater than 1.5 m is likely be affected by the skin friction along the rod in the soft clay above that depth, as discussed earlier. Hence the results of KPT and SASW tests were not considered contradictory, if not in clear agreement. More importantly, the SASW tests indicated the presence of compacted dyke fill, the crust and a similar thickness of soft clay as determined from the field vane shear tests.

3. INSTRUMENTATIONS

The instruments installed at the site are shown in Figure 8, including 13 tensiometers (Kasetsart University or KU-type), 2 flushable tensiometers (UNSUC), 3 MPS suction sensors, 3 Time Domain Reflectometry moisture sensors (TDR), 1 tipping bucket rain gauge, and 1 interval camera. Settlement plates have been installed on the slope at 7 locations (SP1 to SP7). The details of these instruments regarding installation depth and location are summarized in Table 3.

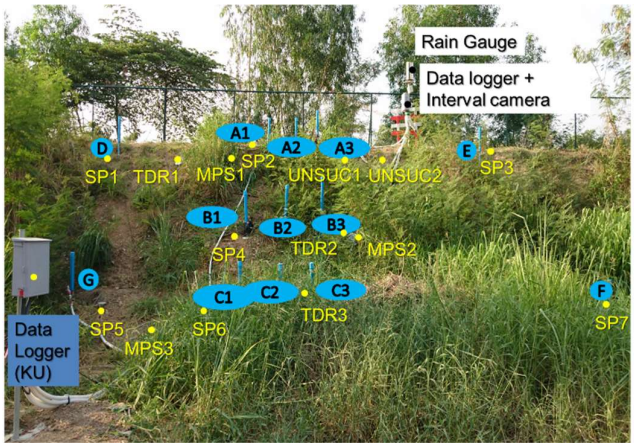

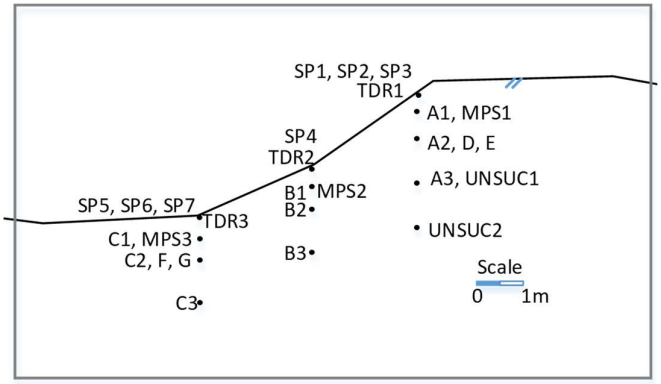

Figure 8 Location of instruments and survey points

Table 3 Summary of instrumentation

Instrument	Instrument code	Depth of installation, m, or location	Measurement working range
Tensiometer (KU-type)	A1, A2, A3 B1, B2, B3 C1,C2,C3 D, E, F, G	0.5, 1, 2 0.5, 1, 1.7 0.5, 1, 2 1	Pore-water pressure -80 to 600 kPa
Tensiometer (Flushable)	UNSUC1 UNSUC2	2 3	Pore-water pressure -80 to 80 kPa
MPS suction sensor	MPS1, MPS2, MPS3	0.5	Pore-water pressure -9 to -1,000,000 kPa
TDR moisture sensor	TDR1, TDR2, TDR3	0.1	-
Tipping bucket rain-gauge	RG	Top of dyke	-
Interval camera	I-cam	Top of dyke	-

Most of the monitoring devices were installed on 17-18 March 2017. The pore water pressures, both positive and negative (i.e. matric suction) values, were measured by three different types of sensors. One of them, the Kasetsart University (KU)-type tensiometer was developed by Jotisankasa et al., (2007) using MEMs pressure sensors and 1-bar air-entry ceramic filter, as shown in Figure 9.

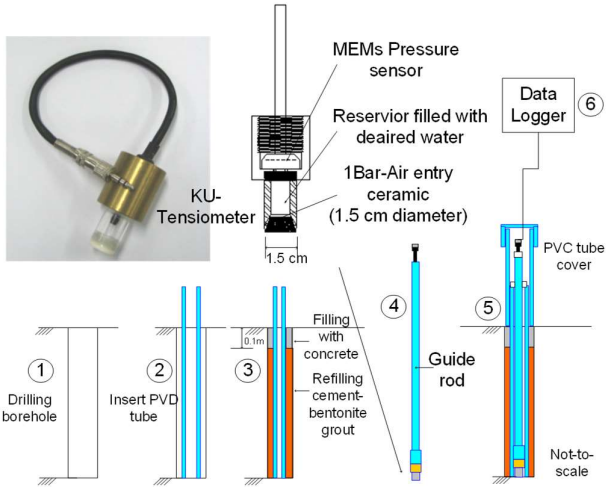

Figure 9 KU-tensiometer and the installation method

The KU-tensiometers were installed at various locations (A1, A2, A3, B1, B2, B3, C1, C2, C3, D, E, F, and G) from depths of 0.5 to 2 m along the slope as shown in Figure 8. The installation procedure of KU tensiometers is described in Figure 9. First, a hole was created by hand auger and pipe driving to the required depth. Afterwards, a PVC casing was inserted down the hole. The tensiometer was then inserted into the PVC casing and a good contact between the tensiometer's ceramic tip and the soil was ensured by checking response by a gentle push in the field. A thin layer of clay paste was also applied to the ceramic tip to improve contact condition. Any gap between the tube and drilled hole was backfilled with cement-bentonite-kaolin grout. It was always ensured that the tensiometer was well saturated with water and no air bubble was present in the reservoir by checking suction reading before installation. After some time during the monitoring period, if the reading suggested that the suction could be higher than 80 kPa and the air-bubble may form inside water reservoir, the KU-tensiometer would then be removed from the borehole through the PVC tube, up to the ground, for checking and re-filling with water later.

The KU tensiometers were supplemented by another type of tensiometers, flushable Mol UNSUC ML-2400AEL (Figure 10), which were continuously buried at 2 m and 3 m depths from the top of the dyke. These UNSUC tensiometer employs tubing connected to the water reservoir for flushing air out of the system and can be resaturated without removing the tensiometer from the borehole. These two types of tensiometer both adopt the conventional principle of tensiometry by using high air-entry value ceramics and are prone to cavitation in the water reservoir below -80 kPa of pore water pressure.

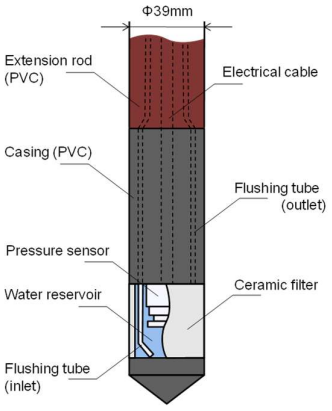

10 UNSUC-tensiometer

These tensiometers were flushed whenever cavitation was detected as indicated by the suction readings. The frequency of tensiometer maintenance depends on the location and the depth of installation. For example, UNSUC tensiometers were flushed twice during the rainy season when suction reading suggested cavitation had occurred. During the prolonged dry season, re-saturation of the tensiometer was not attempted, since the tensiometer always cavitated after re-saturation due to the ground's high suction. The other type of device, Decagon MPS6 (Figure 11a) works on a different principle and has a much wider measurable range of suction. They measure the electrical capacitance of the ceramics that is in direct contact with the soil and hence changes its retained water volume in equilibrium with the soil's suction. Inevitably, this principle implies that the suction measurements are subject to the hysteresis of the ceramics' water retensivity. Three MPS6 were installed at 0.5 m depth, each of which at the shoulder, middle and toe of the slope (Figure 8).

The surface moisture condition was monitored by TDR (Time Domain Reflectometry) soil moisture sensors (Campbell C-CS655-9.9, Figure 11b) with a 120 mm probe length, measuring the volumetric water content over the same thickness of the surface soil. Similarly to MPS6, each of them was installed at the shoulder, middle and toe. The rain gauge was a conventional tipping bucket type with a resolution of 0.5 mm. It was installed further away from any tree canopy and there was nothing overhead that could cause adverse effect on accuracy of the rain gauge. The interval camera recording was taken every hour.

The rain gauge, TDR, MPS and flushable tensiometers readings are recorded by a Campbell-Scientific datalogger at the interval of 1 hour. The KU-tensiometer readings were recorded using a laboratory-made Arduino datalogger (with 16bit ADU) at the interval of 5 minutes. Atmospheric pressure was also measured by an absolute pressure sensor in order to correct for zero-reading of the pore-water pressure from the tensiometers.

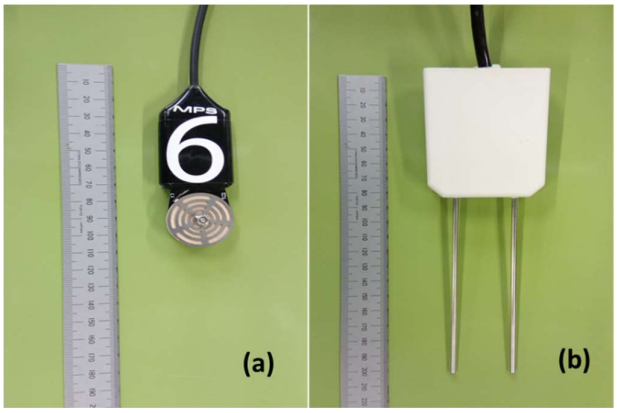

Figure 11 Other instruments for suction and moisture content measurements: a) MPS water potential sensor (Decagon MPS-6), and b) TDR (C-CS655)

4. PORE-WATER RESPONSES AND DYKE MOVEMENTS

4.1 Rainfall pattern

The complete instrumentation program started from April 2017, which was near the end of dry season in Bangkok, up until the present. In this paper, the monitoring results up until July 2017 are presented which encompassed the rain season. The daily rainfall and cumulative rain during the measurement period are presented in Figure 12. The daily rainfall was plotted together with the 3-day antecedent rain in Figure 13a and compared with a critical rainfall envelope (100 mm) which is the commonly used criterion for rainfall-induced slope instability warning in Thailand (Mairaing et al., 2012). The 3-day antecedent rainfall was used according to studies by Thaiyuenwong

(2009) and Mairaing & Thaiyuenwong (2010), which suggested that this antecedent period was suitable for landslide warning in Thailand. No major failure however was observed at the studied site despite the rainfall data crossing the 100 mm rainfall envelope. The hourly rainfall is also plotted against the 24-hour rain in Figure 13b. It can be seen that for the case of total 24-hour rain exceeding 40 mm, the hourly rainfall was nearly equal to the 24-hour rain, indicating nearly all amount of rain within 1 day took place only within 1 to 2 hour period of intensive rain. In fact, based on the rain data, there was a 66% chance that on a rainy day, an hourly rain within that day would be equal to 50% or more of the total 24-hour rain.

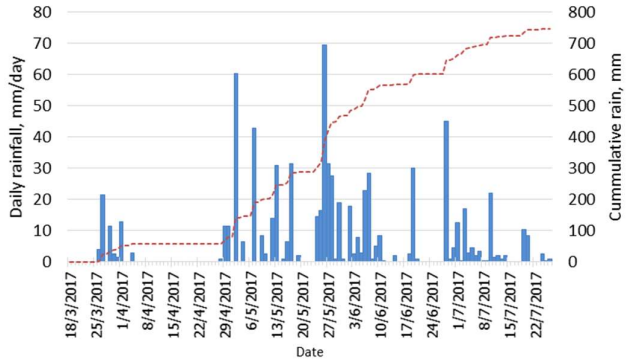

Figure 12 Daily rainfall and cumulative rain during the monitoring period

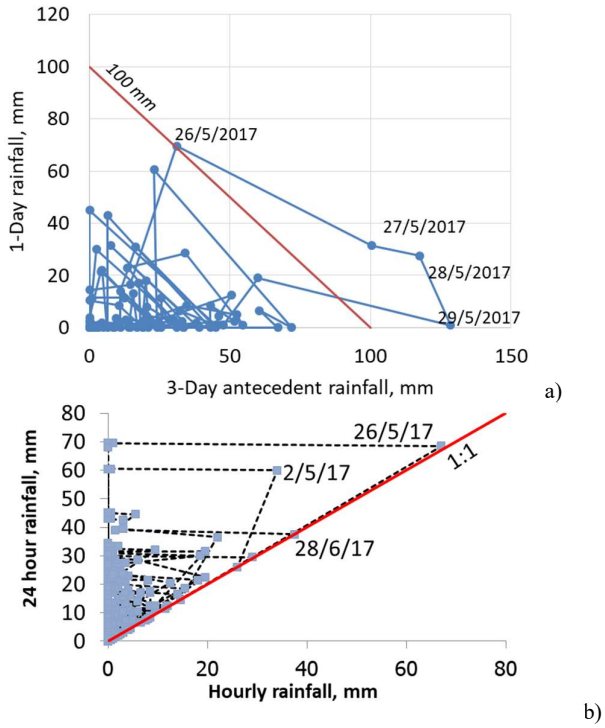

Figure 13 Rainfall pattern during measurement period

4.2 Pore-water pressure, suction and moisture content

The variations of pore-water pressure with time at crest, middle part, and toe of the dyke are shown in Figures 14, 15 and 16 respectively. Highly negative pore-water pressure (high suction) could be observed from April until the beginning of May 2017 which was the drought period. A comparison between pore-water pressures from MPS suction sensor and KU-tensiometer which were installed at the same depth of 0.5 m was made. The MPS sensors suggested pore-water pressure steadily decreased during drought period to about -700 and -2000 kPa, while most KU-tensiometers could only measure pore-water pressure down to about -50 to -90 kPa before cavitation occurred. These KU-tensiometers were then resaturated with deaired-water on 17 May 2017 after which the results were more reliable and thus shown in the Figure. There appeared to be a constant deviation between MPS and tensiometer readings during the rainy season (i.e. between sensors MPS1 and A1 in Figure 14; MPS2 and B1 in Figure 15; MPS3 and C1 in Figure 16). This deviation varied from 5 to 15 kPa and was believed to be caused by hysteresis in MPS suction measurement. The manufacturer of MPS sensor also claimed the device to work reliably from -9 to -1,000,000 kPa, and would not be suitable for a near saturation condition. Accordingly, during the drought season, interpretation of pore-water pressure at 0.5 m will be done only from MPS readings and not from tensiometers. During the rainy season when the suction was below 100 kPa, the readings from tensiometers were considered more reliable and the MPS readings were omitted in the analysis.

A comparison between UNSUC- and KU-tensiometers was also made for measurement at 2 m depth in the crest of dyke (UNSUC1 and A3 in Figure 14c). During drought period in April 2017, both devices could not measure the suction reliably since the value exceeded 100 kPa and both sensors were prone to cavitation. Nevertheless, there was discrepancy between the pore-water pressure readings of the two kinds of tensiometer during rain period (May until July 2017). While the KU-tensiometer indicated negative pore-water pressure gradually increasing from -70 to -60 kPa during the rain, the UNSUC-tensiometer suggested near zero pore-water pressure which was quickly responsive to the rain event. The locations of two sensors (UNSUC1 and A3) were only about 1 m apart and the difference in ground condition was unlikely. It was thought that the UNSUC's fast response was not indicative of the likely low permeable of the fill and could be caused by imperfect sealing around the borehole and sensor rod at the time of installation. The UNSUC2 measurement at 3 m suggested a relatively constant negative pore pressure (-10 kPa), which was slowly increasing with time, a similar behaviour to A3 tensiometer.

By comparing readings from tensiometers installed at the same depth of 1 m but different locations (i.e. between D, E, and A2 in Figure 14; and F, G, and C2 in Figure 16), in general, a consistent measurement of pore-water pressure could be observed with a deviation of about 5 kPa. Point E tensiometer appeared to dry faster than Point D and A2 tensiometers during 17 until 27 May 2017. This could be due to inherent non-uniformity of the evapotranspiration process, and still could not be fully explained at the moment. The overall trend in Figure 14a suggests that the upper layer (surface to 1 m depth) of the dyke crest had a faster response to pore-water pressure change due to rain event. The readings from the lower silty fill (A3) and the crust zone (UNSUC2) appeared to have slower response in pore-water pressure (Figure 14c). The pore-water pressure behaviour at the middle and toe of the dyke (Figures 15 and 16 respectively) also showed a slower response. It is noteworthy that the road surface mainly consisted of granular material (Figure 2 and Table 1), while the lower fill and crust were of higher fine content. Although the pore water pressure responses are expected to be fast at shallower locations even in a uniform dyke, the comparison between the same depth from the shoulder and middle/toe suggests that the difference in soil types and permeability of the road surface could also play an important role.

The variations of volumetric moisture content from TDR sensors are shown in Figure 17. The response of the surface moisture content to climate (i.e. rainfall and evaporation) was expectedly more immediate than the response of pore-water pressure at greater depth. The values of moisture content in Figure 17a was obtained from the manufacturer's calibration information and thus subject to uncertainties in their calibration database. Therefore, the three data series were then normalized by their own maxima, based on the assumption that the maxima correspond to full saturation, and converted into the degree of saturation as shown in Figure 17b.

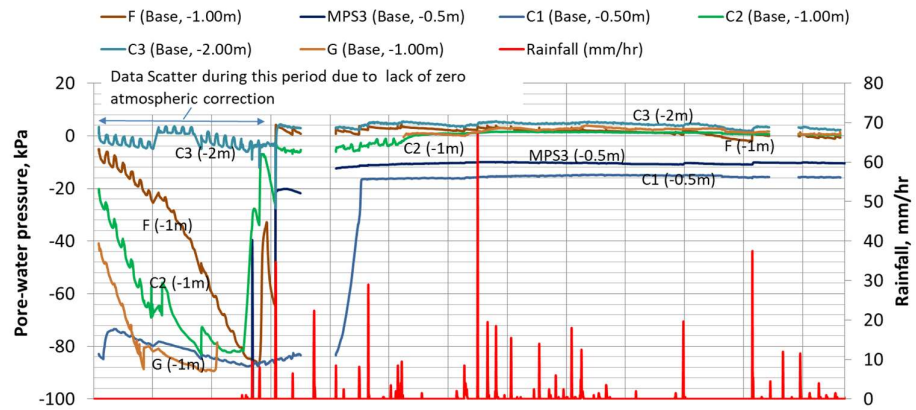

a)

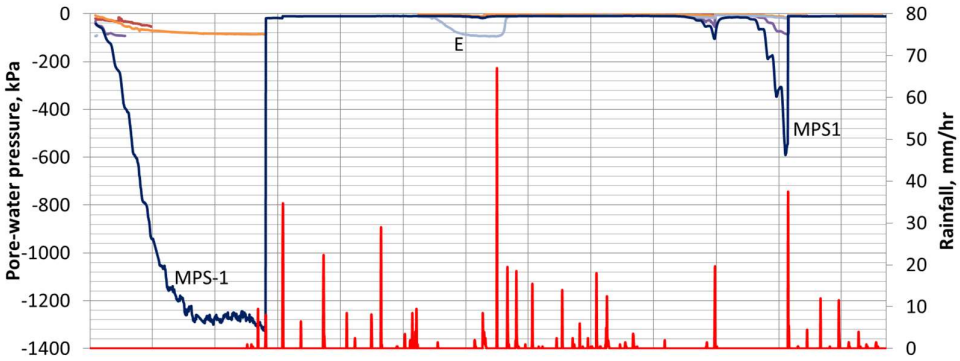

b)

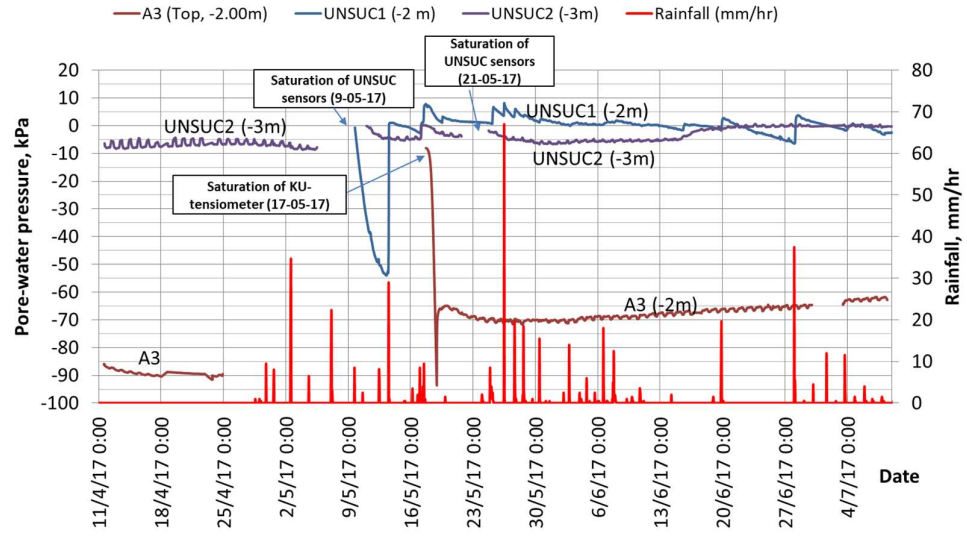

c)

Figure 14 Pore-water pressure along the vertical line from the upper part of dyke: Plot a) and b) pore-water pressure at depths of 0.5 and 1 meter; Plot b) is a reproduction of Plot a) in wider vertical axis range; Plot c) pore-water pressure at depths of 2 and 3 meter

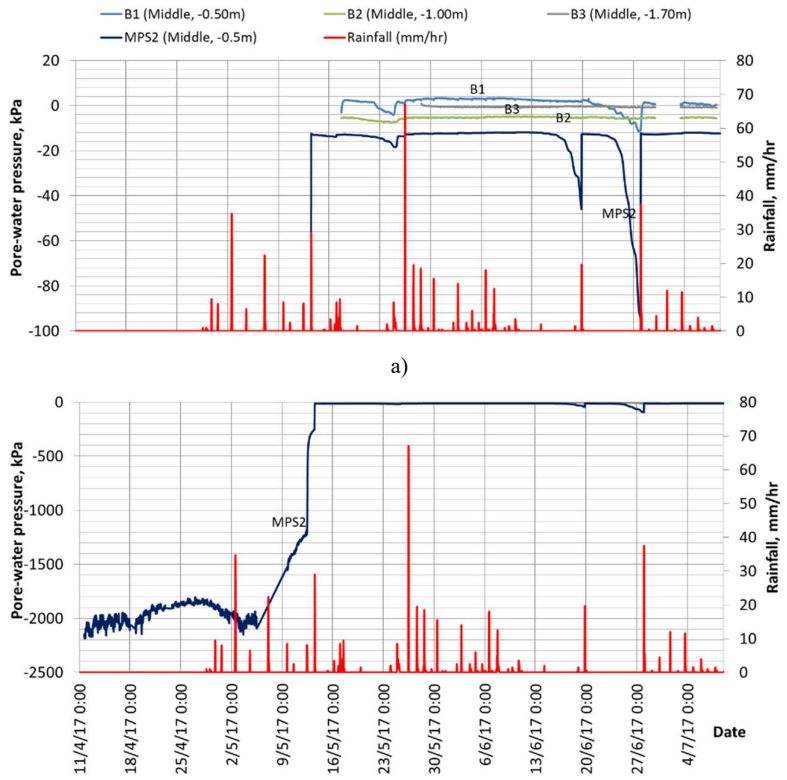

Figure 15 Pore-water pressure along the vertical line from the middle slope part of dyke: Plot b) is a reproduction of Plot a) in wider vertical axis range

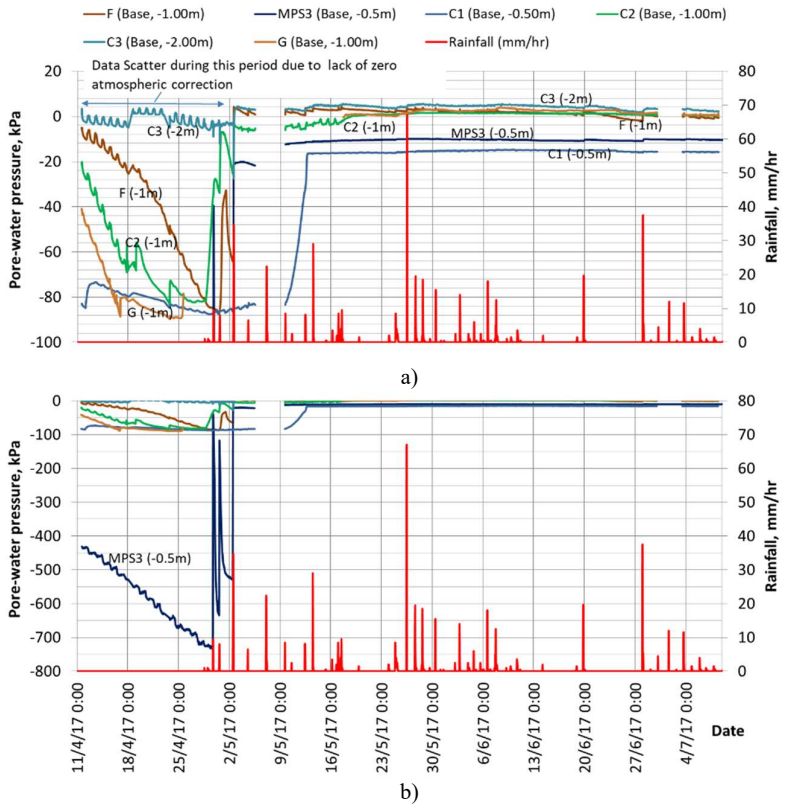

Figure 16 Pore-water pressure at the toe of dyke: Plot b) is a reproduction of Plot a) in wider vertical axis range

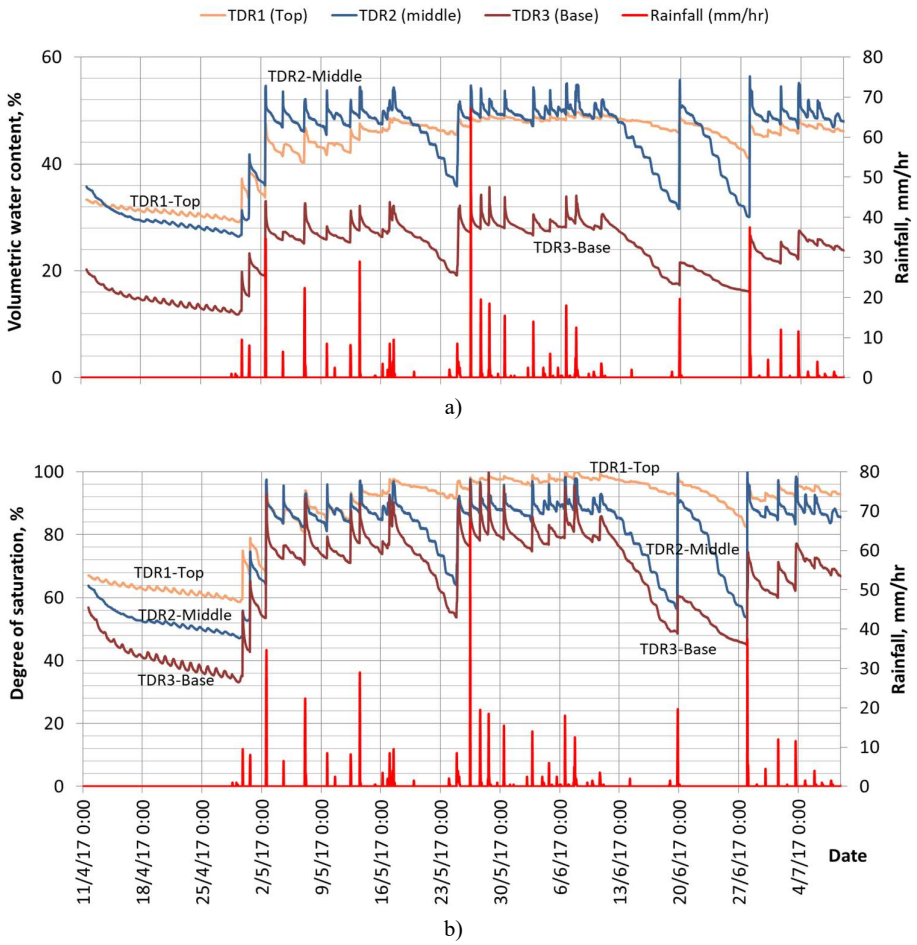

Figure 17 Variation of a) volumetric moisture content and b) degree of saturation at the surface with time

The degree of saturation at the middle part (TDR2) and the toe (TDR3) appeared to decrease at a greater rate than that at the dyke crest (TDR1). The increase in degree of saturation due to rain events appeared to be of greater magnitude at the toe and the middle part too. The reason for this is unclear but could be related to the thicker vegetation observed nearer the dyke toe. Root-inclusions and transpiration from grasses could play an important role in surface moisture content change in this respect.

The pore-water pressures contours of the dyke were drawn based on measurements on 27 April, 27 May and 27 June 2017, as shown in Figure 18. In preparing these contour plots, unreliable measurements (i.e. readings when cavitation occurred, or borehole sealing was not perfect) were excluded. Apparently, the drought period in the year 2017 brought about highly negative pore-water pressure (suction) in the dyke, especially the upper 2 m where the suction reached values between 100 and 1800 kPa in late April (Figure 18a). The subsequent rainfall in May 2017 caused the dyke to become wetter with suction ranging between 10 to zero kPa (Figure 18b) near the surface, as a result of infiltration and groundwater rising. The groundwater table appeared to be higher near the toe than in the middle, possibly due to the influence of the external water level in the pond. At the end of May 2017, the centre part of the dyke still appeared dry with a suction value of 60 kPa, indicating the gradual infiltration and seepage process due to relatively low permeability of the soil.

Further rainfall events in June 2017 caused the groundwater level to rise (Figure 18c). The groundwater in the centre was slightly higher than at the toe, perhaps in response to the infiltration water recharging the groundwater table or due to the external water from outside of AIT. It can be seen that upper part of dyke crest was drier now with suction of nearly 600 kPa in response to the no-rain period from 20 until 27 June 2017. This indicated that the drying process took place first at the crest of the dyke as a result of gravimetric drainage. In addition to this, there was no ground cover and evaporation would have taken place more quickly.

4.3 Dyke surface movement

Surface movement of the dyke was monitored by means of Total Station surveying. Two permanent benchmarks were constructed on the piers of nearby bridge which were assumed to be stationary. These benchmarks were used as reference points for the Total Station device. The measured coordinates (x, y, z) of all the settlement points (SP1 to SP7) were then used to calculate the vertical and horizontal movements as shown in Figure 19.

The Total Station surveys were made on 18 April, 9 May, and 27 July 2017. The vectors of the surface movement were calculated based on the initial conditions on 18 April 2017. Therefore, the first increment of the vector represented the movement that was caused by the first period of rain which took place between the end of dry season and the first week of May. The toe surface showed some heaving of less than 0.5 cm while the crest of dyke appeared to settle by about 0.5 to 1.5 cm. The middle part of the dyke experienced negligible settlement. Since the first measurement period (from 18 April to 9 May 2017) involved both drying and wetting, the first settlement could be related to both desiccation compression as well as collapse-on-wetting phenomena.

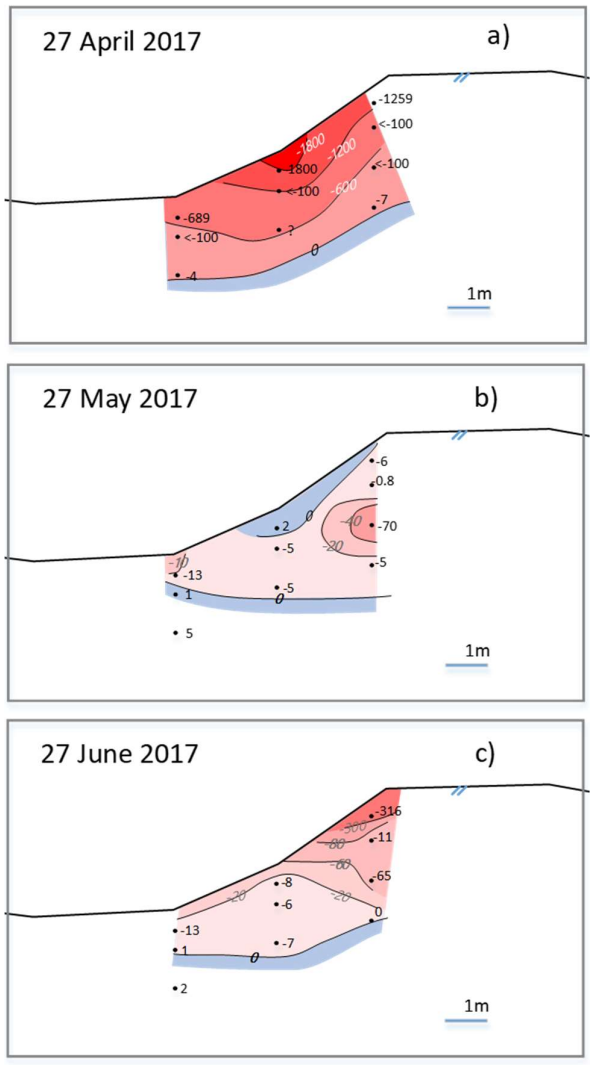

Figure 18 Pore-water pressure contours at three selected dates (the scales are in meter and the contour values are in kPa)

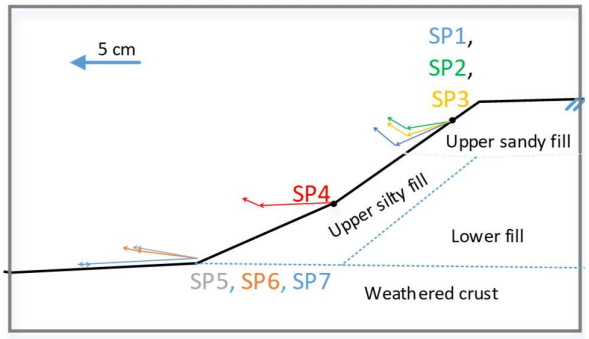

Figure 19 Dyke surface movement

The second vector increments of movement, however, show that nearly all settlement points along the dyke swelled by about 0.5 to 1 cm during the wetting period from 9th May until 27th July. It is noteworthy that the horizontal movements were constantly outwards and their magnitude appeared to be considerable, ranging from 3 to 6 cm. This magnitude of movement seemed excessive and perhaps be affected by the accuracy of horizontal movement from the Total Station survey itself. The first increments of Vectors SP1, SP2 and SP3 nevertheless appeared to be downwards at an angle similar to the boundary between upper and lower fills. The movement at the toe (SP5, SP6 and SP7) also seemed to be mainly horizontal. Although not conclusive, this trend seems to indicate that the movement may primarily take place in the upper fill. This upper fill was also the zone of smaller shear resistance and where pore-water pressure changed to the greater extent. However, the surface movement could also be attributed to the creeping movement of the soft clay foundation soil, though this cannot be fully proven at the moment. The photographs at different periods from the interval camera (Figure 20) did not show a clear sign of exacerbating longitudinal crack along the crest. Yetable 1t, it was quite difficult to confirm the movement based on the interval camera photo alone since the vegetation became thicker during the rainy season. All in all, the movement of the dyke appeared to be related to the change in pore-water pressure and likely be related to the upper part of fill that was recently placed.

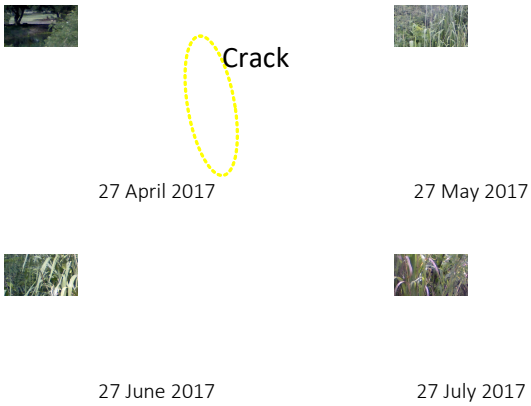

Figure 20 Photos of the dyke crest from fixed-point interval camera

5. CONCLUSION

A field study was undertaken of an instrumented dyke on soft Bangkok clay in Pathumthani, Thailand. The studied site was characterised using dynamic cone penetration tests, field vane shear tests and Spectral Analysis of Surface Waves (SASW) geophysical tests. The pore-water pressure, suction, moisture content and rainfall were continuously monitored over the rainy season in 2017. Based on site characterisation and field monitoring results, the following conclusions can be drawn.

- The thickness of the soft Bangkok clay layer appeared to be only 3.5 to 5m beneath the dyke. The soft clay nearer the dyke was of higher strength than in the zone further away. This was a result of consolidation after the original dyke was built about 50 years ago, and the additional fill was placed in 2012.
- The MPS soil moisture sensors, which employed indirect method for suction measurement, based on electrical capacitance of the ceramics, appeared to be suitable for high suction (>100 kPa). Nevertheless, the MPS sensor was prone to accuracy problem due to hysteresis when measuring small suction. On the other hand, the tensiometers yielded a more accurate measurement during the rainy season, yet not possible to measure the suction of the dyke during dry season due to the cavitation problem.
- The vegetated dyke slope surfaces (50 cm) made up of silty and clayey soils were found to experience drastic suction changes under tropical climate, reaching 1800 kPa towards the end of a drought season and abruptly (within a day) recovering to 20-40 kPa upon the onset of the rainy season. Such large and abrupt changes of the surface suction were likely to have aggravated the surface cracking and hence the dyke movements. On the contrary, the response at 3 m depth from the dyke shoulder was almost insensitive to the short-term rainfall patterns. These

findings have significant implications for further laboratory hydromechanical investigation.

- The toe surface of dyke showed some heaving of less than 0.5 cm while the crest of dyke appeared to settle by about 0.5 to 1.5 cm during the first week of rainy period. The second measurements of movement however showed that surface of the dyke swelled by about 0.5 to 1cm during the wetting period from 9 May until 27 July. This observation suggested that the vertical movements partly reflected an elasto-plastic compression-swelling phenomenon due to combined effects of drying, collapse-on-wetting and swelling and that some deformations were recoverable. This was not the case for the horizontal movements, which exhibited constant outwards cumulative displacement.
- The first increments of displacement vectors at the shoulder appeared to be at an angle similar to the boundary between upper and lower fills. The movement at the toe appeared mainly horizontal. Although not conclusive, this trend seemed to indicate that the movement may have primarily taken place in the recently placed upper fill.

6. ACKNOWLEDGEMENTS

The authors are grateful to the financial support provided by JSPS KAKENHI Grant Number 16H04405, and Kasetsart University Research and Development Institute (KURDI). The authors also would like to thank Dr. Noppadol Phienwej for providing information and comments on AIT dyke. The second author is grateful to the Ministry of Research, Technology and Higher Education, Republic of Indonesia and the Indonesia Endowment Fund for Education (LPDP) scholarship which support his PhD study. The assistance from staffs and students of Geotechnical Engineering Division at Department of Civil Engineering, Kasetsart University, Asian Institute of Technology, and Ecole des Ingénieurs de la Ville de Paris during field works are gratefully acknowledged.

7. REFERENCES

Ashford, S.A., Jakrapiyanum, W., Lukkanaprasit, P. (1996) Amplification of Earthquake Ground Motions in Bangkok, Asian Institute of Technology Research Report. Submitted to the Public Works Department, Thailand.

Duc, D.M, Hieu, N.M., and Lan, N.C. (2017) "Climate change impacts in a large-scale erosion coast of Hai Hau District, Vietnam and the adaptation". Geotechnical Engineering, 48(1), 12-25.

Fern, E.J., de Lange, D.A., Zwanenburg, C., Teunissen, J.A.M., Rohe, A. & Soga, K. (2017) "Experimental and numerical investigations of dyke failures involving soft materials", Engineering Geology, 219, 130-139.

Jasim, F.H. & Vahedifard, F. (2017) "Fragility curves of earthen levees under extreme precipitation", Geotechnical Special Publication, pp. 353.

Joh, S.-H. (1996) "Advances in Interpretation and Analysis Techniques for Spectral-Analysis-of-Surface-Waves (SASW) Measurements", PhD. Dissertation, The University of Texas at Austin.

Jotisankasa, A., Mahannopkul, K. & Sawangsuriya, A. (2015) "Slope stability and pore-water pressure regime in response to rainfall: A case study of granitic fill slope in northern Thailand", Geotechnical Engineering, 46(1), 45-54.

Karl, L., Fechner, T., François, S., & Degrande, G. (2008). Application of surface waves for the geotechnical characterisation of dykes. Paper presented at the Near Surface 2008 - 14th European Meeting of Environmental and Engineering Geophysics

Mairaing, W. & Amonkul, C. (2010) "Soft Bangkok clay zoning" EIT-Japan Symposium on Engineering for Geo-Hazards: Earthquakes and Landslides-Surface and Subsurface Structures, Bangkok, Thailand, September 6-7, 2010.

Mairaing, W. & Thaiyuenwong, S. (2010) "Dynamic landslide warning from rainfall and soil suction measurement" Proceedings of the International Conference on Slope 2010 : Geotechnique and Geosynthetics for Slopes, 27-30 July, 2010 Chiangmai, Thailand.

Mairaing, W., Jotisankasa, A. and Soralump, S. (2012). "Some applications of unsaturated soil mechanics in Thailand: an appropriate technology approach". Geotechnical Engineering Journal of the SEAGS & AGSSEA, 43(1), 1-11.

Nazarian, S., Stokoe, K.H.II and Hudson, W.R. (1983) "Use of Spectral Analysis of Surface Waves method for determination of moduli and thicknesses of pavement systems", Transportation Research Record, 930, 38-45

Nishimura, S., Tokoro, T., Yamada, T., Izumi, N. and Rivas, M. F. (2015). "A case study of long- and short-term hydraulic state changes in embankment in Hokkaido", Proceedings of 6th Japan-China Geotechnical Symposium, JGS Special Publication, 1(7), 34-39.

Robinson, J.D. & Vahedifard, F. (2016) "Weakening mechanisms imposed on California's levees under multiyear extreme drought", Climatic Change, 137(1-2), 1-14.

Sills, G.L., Vroman, N.D., Wahl, R.E., and Schwanz, N.T. (2008) "Overview of New Orleans levee failures: lessons learned and their impact on national levee design and assessment". Journal of Geotechnical and Geoenvironmental Engineering, 1340(5), 556–565.

Stokoe, K. H., Wright, S. G., Bay, J. A., and Roesset, J. M. (1994). "Characterization of geotechnical sites by SASW method, in geophysical characterization of sites." ISSMFE Technical Committee #10, edited by R. D. Woods, Oxford Publishers, New Delhi, 15-25

Thaiyuenwong, S. (2009) "Landslide Hazard Analysis by Geotechnical Engineering Method Considering Dynamic Factors in Andaman Coastal Area of Southern Thailand" PhD thesis, Department of Civil Engineering, Kasetsart University (in Thai).

Tsaparas, I., H. Rahardjo, D.G. Toll and E.C. Leong (2003). "Infiltration Characteristics of Two Instrumented Residual Soil Slopes". Canadian Geotechnical Journal, 40(5), 1012 – 1032.

Van Baars, S. (2005). "The horizontal failure mechanism of the Wilnis peat dyke." Geotechnique, 55(4), 319-323.

Vahedifard, F., Sehat, S. & Aanstoos, J.V. (2017) "Effects of rainfall, geomorphological and geometrical variables on vulnerability of the lower Mississippi River levee system to slump slides", GeoRisk, 11(3), 257-271.

Vahedifard, F., Robinson, J.D. & AghaKouchak, A. (2016) "Can protracted drought undermine the structural integrity of california's earthen levees?" Journal of Geotechnical and Geoenvironmental Engineering, 142(6).